

Genesis and growth of internal microstructures of manganese nodule

V K Banakar

National Institute of Oceanography, Dona Paula, Goa 403 004, India
and

M Tarkian

Institute of Mineralogy and Petrology, University of Hamburg, 2000 Hamburg 13, FRG

Received 30 April 1990; revised 29 November 1990

Microscopic and microprobe studies of manganese nodule from the Somali basin indicate that the reflectance of Fe-Mn oxyhydroxide varies with Mn and Fe concentrations. The non-oxyhydroxide components (detrital, biogenic debris, organic matter, etc.) appear to have a substantial control in the growth of different microstructures and show tendency to align their longest axes in the growth direction of structural units. This alignment appears to be due to the inward forces associated with surface tension of the 2 adjacent colloidal precipitate surfaces which have a tendency to grow into a spheroid, probably similar to phenomenon of drop formation. Detrital components within the nodule material identified include heavy titanium minerals, viz. titanomagnetite, ilmenite and rutile which may be the erosional products of precambrian granites of the Seychelles group of islands. The microprobe point analyses indicate that the studied nodule structures have accreted mainly by hydrogenous precipitation with < 15% detrital influence. The alkali and alkaline earth metals (Na, K, Ca and Ba) appear to exist in the Mn mineral phase as charge balancing cations or result from the adsorption of seawater cations on the large surface areas for δ -MnO₂.

Ferromanganese nodules are composed of intricate internal structures. Sorem and Fewks¹ and Sorem *et al.*² have recognised the variation in internal microstructures and classified them into 4 categories, viz. columnar, mottled, lamellar and compact zones. The microstructures are the fundamental structural units of ferromanganese nodules and crusts and they reflect the environment of genesis and development³. In this paper, internal microstructures of a nodule from the Somali basin are discussed with respect to their genesis.

Materials and Methods

The nodule studied was collected from EEZ of Seychelles (lat. 6°S, long. 52°E) by a Preussag free-fall grab during cruise 135 of *R V Gaveshani*. The nodule is spheroidal and highly compact with very smooth grained surface. It was sliced through the nucleus, cut into rectangular slab, soaked in araldite, vacuum impregnated and polished for microscopic studies using Ziess reflected light microscope. The microprobe analyses for metals present in ferromanganese oxyhydroxide layers were carried out at 4 points on Cameca Camebax microprobe.

Results and Discussion

The structural zones are sharply defined (Fig. 1). Fig. 1A shows a sharp termination of pillar growth into a thin compact zone (at 5.5 mm depth in nodule) of about 60 μ m. This compact zone abruptly ends and leads to another zone of pillar structure. Similarly another structural change can be observed at a depth of 7.1 mm (Fig. 1B) i.e. columnar structure changing into a fibrous type of layering. The columnar or pillar structure indicates slow and steady supply of metal hydroxides from overlying water column (hydrogenous precipitation). Another notable feature in this figure (1A) is the varying dimensions of pillars. The pillars above the compact zone are nearly half the size of the pillars below compact zone. The reason for such microstructural variation might be due to the difference in supply rate of oxyhydroxide colloidal flocs from the water column during a short span of their growth history. Large well developed pillars below the compact zone indicate a higher supply rate of metal oxyhydroxide and lower supply of non oxyhydroxides. The compact zone might have developed due to a short lived episode of comparatively very high metal oxyhydroxide supply with insignificant detritus input. Co-

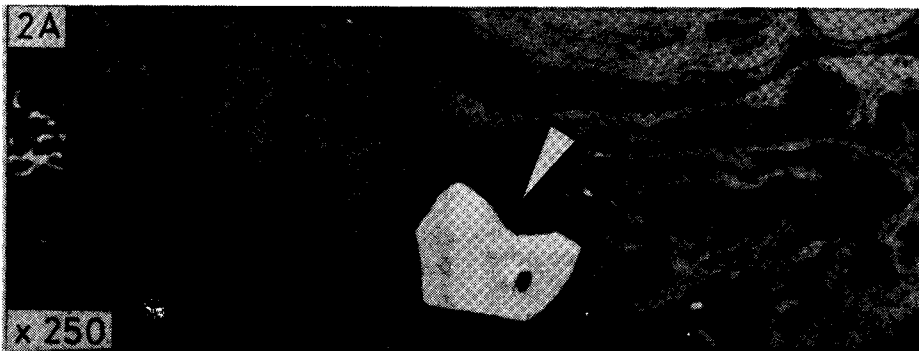
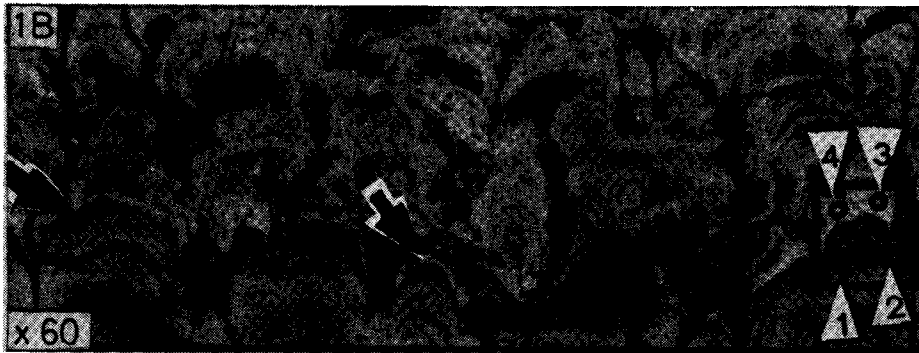


Fig. 1-A - Thin compact zone separating 2 generations of pillar zones. B - Transition of lower reflectance columnar zone into slightly higher reflectance fibrous type of chaotic layering above [The marked area is studied for microprobe point analyses. The arrows with numbers indicate the points analysed]

Fig. 2 - High reflectance detrital grains (arrows) spread all over the section [Size of these detrital grains varies from few μm to $80 \mu\text{m}$. A - Titanomagnetite ($75 \mu\text{m}$) with small inclusion of pyrrhotite (high reflectance) at the centre of photograph. B - Elongated crystal of ilmenite ($20 \mu\text{m}$) at the centre of photograph]

lumbar and pillar structure indicating slow growth rate and compact and mottled structure indicating fast growth rate⁴ can be related to changes in depositional environments during the accretion of nodule⁵. Similar structural changes in Pacific crusts have been related to variations in depositional paleoenvironments⁶.

The observed structural variation at 7.1 mm depth can be explained as due to sudden turnover of nodule, probably as a result of biological activity in the underlying sediment substrate⁷ which exposes hydrogenetically accreting surface to probable diagenetic source and *vice versa* or a sudden increase in sedimentation⁵.

Microscopic and microprobe studies show abundant presence of high reflectance Mn bearing Fe-Ti oxide minerals as small crystals (up to 80 μm) of haematite, titanomagnetite, ilmenite and rutile within or around the oxyhydroxide spheroids (Fig. 2). These detrital grains might be the erosional products of the Seychelles group of granitic islands which are dated to be of late pre-Cambrian period⁸. The titanomagnetite (Fig. 2A) contains up to 0.7% Ti and 0.3% Mn. Ilmenite (Fig. 2B) contains up to 4.6% Mn, which is unusually high. The high content of Mn in ilmenite may be due to the substantial substitution of Mn^{+2} for Fe^{+2} leading to a Mn rich end member pyrophenite which is a very rare mineral⁹. Rutile contains up to 1% of Mn which is also unusually high considering very limited scope for Mn substitution for Ti indicating its genesis probably as an alteration product of pyrophenite.

The microprobe investigations at 4 points, marked in Fig. 1B (1 and 2 at lower reflectance portion and 3 and 4 at slightly higher reflectance portions), indicate comparatively higher Mn concentration in higher reflectance area than in lower reflectance area (Table 1). Fe shows the opposite behaviour.

The interelemental correlation based on 4 point analyses (though statistically not significant) show a strong positive correlation between alkali and alkaline earth metals (Na, K, Ca and Ba, > 0.9) and a negative relation with Mn. Electron spin resonance studies of crusts and nodules by Pattan and Mudholkar¹⁰ have shown the presence of Mn^{+2} in hydrogeous crusts and nodules from the Central Indian Basin. Ca, K, Na, Ba might therefore have been incorporated into the Mn mineral phase as charge balancing cations in preference when the availability of other transition metals is low¹¹. The concentrations of alkali and alkaline earth metals in the analysed points increase with decreasing transition metals. Mn/Na + Ca + K + Ba shows a large variation from 7.6 (at point 1) to 93.2 (at point 4). Mn/

(Cu + Ni + Co) on the other hand shows nearly a constant ratio of ~ 15 for all 4 points. This can be due to the increasing uptake of transition metals with increasing Mn and decreasing uptake of alkali and alkaline earth metals with increasing Mn, Co, Ni and Cu in the nodule mineral structure. Hence, the alkali and alkaline earth metals might be present in the analysed microstructural units as charge balancing cations rather than in association with detrital material. This inference is derived from the very poor correlation of these metals with Si and Al which have detrital source or with Fe-hydroxide. The incorporation of these metals due to the adsorption on large surface area of $\delta\text{-MnO}_2$ is also a possibility¹². Co and Ni show very strong negative relation with Fe (> 0.9) and strong positive relation with Mn (> 0.8) which is the general behaviour of these metals in hydrogenetic precipitates due to specific adsorption of Co^{+2} and Ni^{+2} by $\delta\text{-MnO}_2$ surfaces¹³.

Near perfect polished sections (Fig. 3A-H) of this nodule when observed with high magnification under ore microscope reveal detailed and complex behaviour of structural units (referred as microbands in foregoing discussion). In general the various structural zones, viz. columnar, pillar, dendritic, compact, etc. appear to be composed of alternate microbands of relatively high and low reflectance. From Fig. 3 it is evident that from the beginning, the growth of structural unit under favourable conditions tends to develop as a spheroid (Fig. 3 A-C and E), similar to the mechanism of formation of a drop. The spheroidal growth of oxyhydroxide colloidal precipitate probably ceases once the space is restricted from the sides or from the base due to simultaneous growth of neighbouring oxyhydroxide spheroids or

Table 1 - Elemental distribution in the analysed points
[All values are in weight percent]

| | Point 1 | Point 2 | Point 3 | Point 4 |
|-------|---------|---------|---------|---------|
| Na | 0.111 | 0.084 | 0.102 | 0.090 |
| K | 0.193 | 0.041 | 0.134 | 0.008 |
| Fe | 17.025 | 17.862 | 17.301 | 15.355 |
| Si | 3.751 | 3.244 | 3.130 | 3.354 |
| Ca | 2.096 | 0.395 | 1.716 | 0.143 |
| Al | 1.631 | 1.271 | 1.205 | 1.527 |
| Ba | 0.594 | 0.119 | 0.351 | 0.047 |
| Co | 0.496 | 0.441 | 0.429 | 0.593 |
| Ni | 0.299 | 0.316 | 0.327 | 0.476 |
| Zn | 0.320 | 0.322 | 0.332 | 0.223 |
| Pb | 0.551 | 0.060 | 0.237 | 0.026 |
| Cu | 0.742 | 0.797 | 0.805 | 0.751 |
| Mn | 22.839 | 23.365 | 24.301 | 26.609 |
| Mn/Fe | 1.340 | 1.310 | 1.400 | 1.730 |

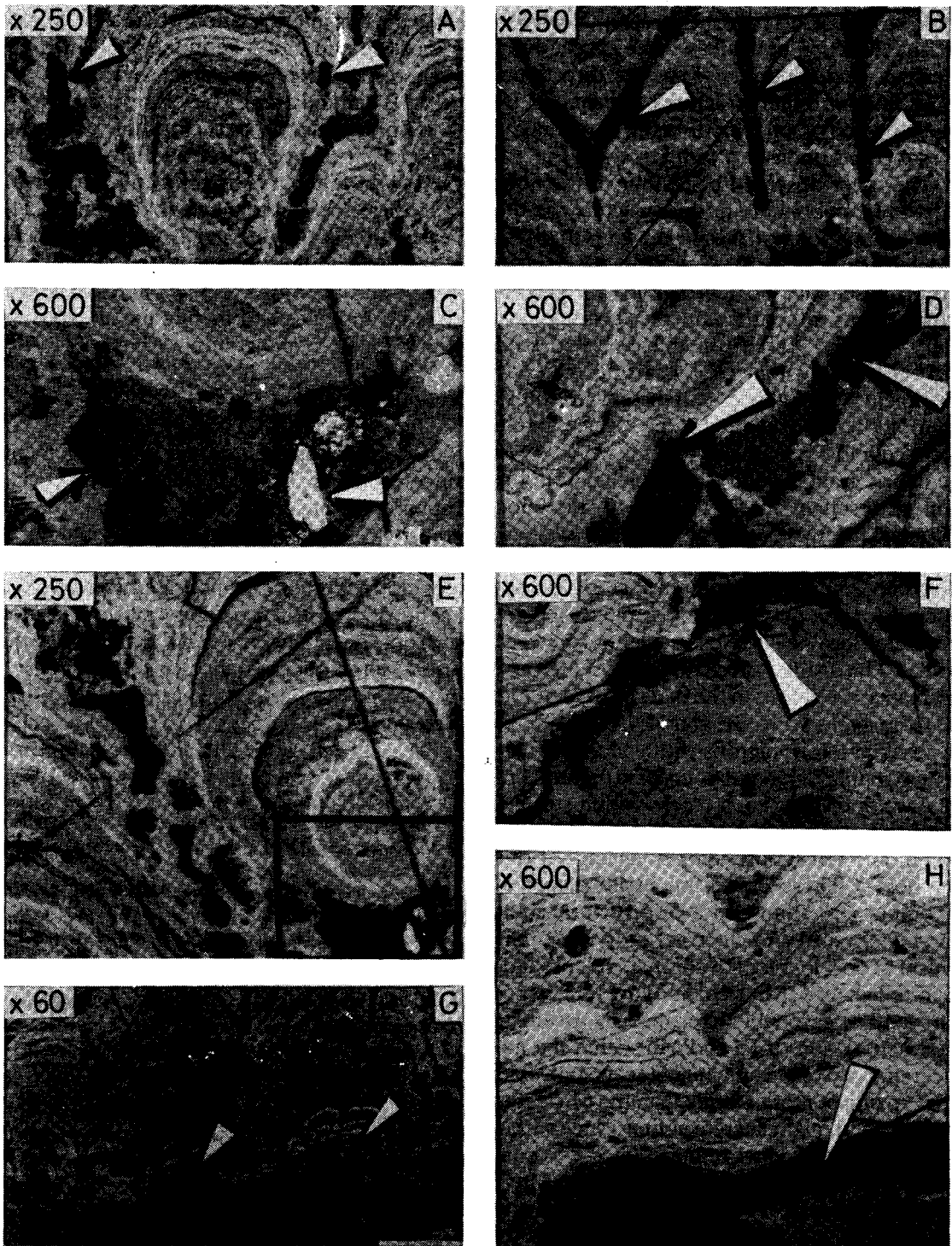


Fig. 3 – Microphotographs showing the various minute features in studied nodule indicated by arrows. A, B, C and E show the tendency of Fe-Mn oxyhydroxide colloidal precipitates to form a spheroid in the beginning. A and B – Arrows indicate the biogenic tubes aligned in the growth direction at the contact of adjacent oxyhydroxide precipitates. C, D and E – Biogenic debris and detrital grains aligned in the growth direction of oxyhydroxide precipitates. F, G and H – Arrows indicate the micro-crack separating two oxyhydroxide precipitates of varying physical and chemical properties(?). The marked area in G and enlarged in F and H show the alternate bands of high and low reflectance oxyhydroxide precipitates

due to interruption by detrital material as shown in the marked area of Fig. 3E (and magnified portion of Fig. 3E in Fig. 3C). Then, the directional growth starts in the direction of available free space (away from nucleus) and continues. Thus the directional growth of internal microstructures appears to be controlled by the non-oxyhydroxide components like detrital grains (indicated with arrows in Fig. 3A and B). The other observed behaviour of the non-oxyhydroxide components in the structures is the alignment of their longest axes in the growth direction of microbands (Fig. 3A-C and D). To explain this, it is proposed that the debris grains are the primary components rather than the post accretionary secondary infilling based on their sealed and trapped behaviour within oxyhydroxide material. This alignment is probably due to the inward forces (due to surface tension) exerted at the surfaces of the 2 adjacent colloidal precipitate systems which try to pull the debris grain (a solid) so as to align it in the direction of resultant force (i.e. growth direction along contact of two adjacent colloidal system). Thus, the non-oxyhydroxide components (may be detrital or biogenic debris) probably act as cementing material for the development of pillars, or columns or dendrites to give rise to structural zones in the nodules. The distinct alternate bands of high and low reflectance are shown in the marked area of Fig. 3G and its magnified Fig. 3F and H. In all these figures a crack of a few microns width (shown by arrows) is separating older and younger structural units. The development of such cracks within structural microbands might be due to shrinking of older precipitate during its consolidation (ageing) or due to water loss¹⁴. These cracks might be planes of weakly bound structural zones or structural units with varying physical and chemical properties. The mechanism of development of alternate microbands with high reflectance (Mn rich) and low reflectance (Fe rich) can be reasonably explained by assuming that the fractionation of Fe and Mn within the nodule accretionary environments¹⁵ is responsible. Since Fe⁺² oxidises more readily than the Mn⁺², the Fe rich dark band might accrete at first. Once within the accretionary microenvironments the Fe⁺² concentration level is dropped due to its removal; Mn⁺² enrichment in the microenvironment increases with respect to Fe⁺² and is followed by oxidation of Mn⁺² to give rise to Mn rich light colour microbands. This process alternates and continues till the growth of nodule ceases. The thickness of microbands thus probably depends upon the enrichment

factor of these 2 metals within the accretionary microenvironments. The microprobe data (Table 1) supports this interpretation where a difference of ~ 4% of Mn and ~ 2% Fe in the analysed points has been responsible for distinct reflectivity variation (Fig. 1B marked area). Therefore, it may be possible to calibrate Mn, Fe concentration with respect to percent reflectance if large number of samples from varying accretionary environments are studied.

The proposed mechanism of alignment of debris in the structural zones needs to be tested under laboratory conditions by creating colloidal precipitation phase under high pressure and low temperature aqueous modules and fluxing the aqueous medium with elongated solid grains.

Acknowledgement

The authors thank Dr. B.N. Desai, R.R. Nair and V. Ittekkot for suggestion and encouragement. They sincerely thank Prof. G.P. Glasby, New Zealand Oceanographic Institute, New Zealand, for critically going through the paper and for valuable suggestions. Mr. P. Stutz and Mrs. B. Corlinisen of Mineralogical Institute of Hamburg University, FRG, are acknowledged for providing polished sections and microprobe analyses. Ms. Flavia Fernandes provided secretarial assistance.

References

- 1 Sorem R K & Fewkes R H, in *Marine manganese deposits*, edited by G P Glasby, (Elsevier, Amsterdam) 1977, 147.
- 2 Sorem R K, Reinhart W R, Fewkes R H & McFarland W D, in *Marine geology and oceanography of the Pacific nodule province*, edited by J L Bischoff, (Plenum, New York) 1979, 475.
- 3 Friedrich G & Weichowski A S, *Mar Geol*, 37 (1980) 71.
- 4 Heye D, *Mar Geol*, 26 (1978) 59.
- 5 Marchig V & Halbach P, *TMPM Tscheermarks Min Petrol Mitt*, 30 (1982) 81.
- 6 Segl M, Mangini A, Bonani G, Hoffman H J, Nessi M, Suter M, Wolfli W, Friedrich G, Plugger W L, Weichowski A & Beer J, *Nature Lond*, 309 (1984) 540.
- 7 Glasby G P, *New Zealand J Sci*, 20 (1977) 187.
- 8 Miller J A & Mudie J D, *Nature Lond*, 192 (1961) 1174.
- 9 Deer W A, Howie R A & Zussman J, *Rock forming minerals: non silicates*, (Longmans, London) 1962, pp. 371.
- 10 Pattan J N & Mudholkar A V, *Chem Geol*, 85 (1990) 171.
- 11 Dymond J K, Lyle M, Finney B, Piper D Z, Murphy K, Conrad R & Piasis N, *Geochim Cosmochim Acta*, 48 (1984) 931.
- 12 Murray J W, *J Colloid Interface Sci*, 46 (1974) 357.
- 13 Halbach P & Puteanus D, *Earth Planet Sci Lett*, 68 (1984) 73.
- 14 Heye D, *Progr Oceanogr*, 7 (1978) 163.
- 15 Huh C A & Ku T L, *Geochim Cosmochim Acta*, 48 (1984) 951.